Modelling Intrinsic Rotation Reversals in JET Plasmas

M.F.F.Nave [1], A.Mauriya[1], M.Barnes[2], F.I.Parra[3], E.Delabie[4], M.Baruzzo[5], J.Ferreira[1], J.Garcia[6], A.Kirjasuo[7], M.Lennholm[8], M.Romanelli[9] and JET Contributors*

EUROfusion Consortium, JET, Culham Science Centre, Abingdon, OX14 3DB, UK

[1] *Instituto de Plasmas e Fusão Nuclear, Instituto Superior Técnico, P1049-001 Lisboa, Portugal*
[2] *Rudolf Peierls Centre for Theoretical Physics, Oxford University, UK*
[3] *Princeton Plasma Physics Laboratory, Princeton, NJ 08540, USA*
[4] *Oak Ridge National Laboratory, Oak Ridge, TN 37831-6169, USA*
[5] *ENEA C. R. Frascati,via E. Fermi 45, 00044 Frascati (Roma), Italy*
[6] *CEA, IRFM, F-13108 Saint Paul Lez Durance, France*
[7] *VTT, Espoo, Finland*
[8] CCFE, Culham Science Centre, Abingdon, Oxon, OX14 3DB, UK
[9] *Tokamak Energy Ltd, 173 Brook Drive, Milton Park, OX14 4SD, UK*
** See the author list of "Overview of T and D-T results in JET with ITER-like wall" by CF Maggi et al. to be published in Nuclear Fusion Special Issue*

INTRODUCTION

Recent experiments in JET studied intrinsic rotation in Ohmic plasmas, which provided the first clear observation of rotation reversals in a large tokamak [1]. Main ion rotation measurements were made in H, D and T plasmas for a large density range that spanned over both the Linear Ohmic Confinement (LOC) and the Saturated Ohmic Confinement (SOC) phases. Both isotope ion mass and density were found to have a large effect on rotation. Here we consider the effect of density. Two rotation reversals were clearly observed for each hydrogen isotope, with rotation profiles changing from peaked to hollow at a density close to the LOC-SOC transition, then to peaked again with increasing density. Most theories for intrinsic rotation attribute the observed rotation to a turbulent redistribution of momentum within the plasma core. For analysis of the effect of the density on the core rotation observed at JET, we focus on one of the turbulence drives, the effect of neo-classical parallel velocity and heat flow on the turbulence [2-5]. Using a version of the GS2 code [6] that includes neoclassical flows, non-linear modeling of rotation profiles has been done for plasmas from the H density scan.

OBSERVATIONS OF INTRINSIC ROTATION IN JET OHMIC PLASMAS

EXPERIMENTAL SET-UP.

Density scans in Ohmic plasmas were performed in low triangularity, divertor, configurations with a toroidal magnetic field B_T = 2.7 T and plasma current I_p = 2.3 MA. The density was varied in steps and toroidal rotation measured during steady state density plateaus (figure 1). Conditions were matched in H, D and T plasmas, with $Z_{eff} \sim 1$, for the study of isotope effects.

Fig.1a - Ohmic Hydrogen Plasma at different densities. (i) NBI blips for charge exchange T_i and rotation measurements (ii) Main ion toroidal velocity on the center and edge, (iii) $\langle n_e \rangle$ is line-averaged electron density from far-infrared interferometer, and T_e is central electron temperature from HRTS.

Fig.1b –(i) q-profile from EFIT, (ii) main ion toroidal velocity profiles at beginning of NBI blip (resolution of 10 ms) showing a hollow and a peaked profile.

OBSERVATIONS OF ROTATION REVERSALS

For all three H isotopes, as the density increased, two consecutive core rotation reversals were observed [1]. At the lowest density the whole plasma rotates in the co-current direction. By increasing the density, co-current rotation decreased with a reversal from peaked to hollow profiles. Further increasing the density leads to restoration of monotonic profiles, co-rotation now increasing as a function of density (figures 2 and 4a). The rotation reversals occur at a radius larger than the sawtooth inversion radius and does not appear to be related to MHD instability.

1st Reversal: The reversal of the rotation shear at low densities is similar to observations extensively studied in D plasmas in devices smaller than JET [7]. It occurs associated with a sudden decrease of grad (n_e) at a density close to the LOC–SOC transition and the change from dominant TEM to ITG turbulence (Fig.3) [1].

2st Reversal: No clear transport event is associated with the return to a co-current regime at higher densities. Peaked profiles are observed in the TEM and the ITG regimes. The data indicates a grad T_e threshold below which co-current is observed (fig. 5 b).

(The critical density for the second rotation reversal, increases with ion mass [1]. This will be discussed elsewhere.)

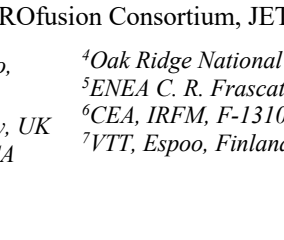

Fig. 2 Central main ion toroidal angular frequency (average over r/a = 0.0–0.3) versus average line density.

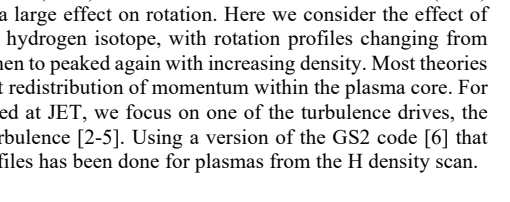

Fig. 3(a) TGLF Linear growth rate, γ, divided by ω, the frequency of turbulence dominant mode, for k ρ_s < 0.8 for radius r/a = 0.6. (b) Thermal energy confinement time, τ_{th}

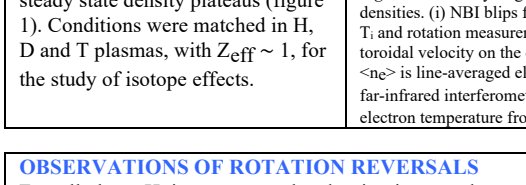

Fig. 4 Normalised rotation shear, at mid-radius r/a=0.5. u'vs <ne>; (b) u'vs Te and u'vs Ti.

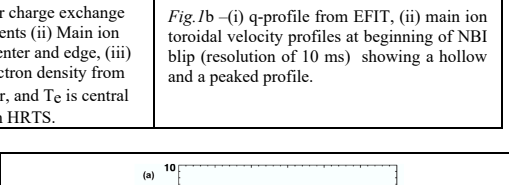

Fig. 5 Rotation shear at mid-radius r/a=0.5 vs scale lengts of (a) electron density a/Lne and (b) electron temperature a/Lte

THE MODEL

Tokamak plasma dynamics typically consist of low amplitude, small-scale turbulent fluctuations on top of a slowly evolving macroscopic equilibrium. In the gyrokinetic approach, the particle distribution function, f, consisting of equilibrium, F, and fluctuating, δf components, is expanded in the small parameter ρ*=ρ/L, where ρ is the ion Larmor radius, and L a characteristic system size. If only the lowest order system of equations for δf is considered, these equations possess a symmetry that prohibits momentum transport in non-rotating plasmas. In order to study intrinsic rotation, higher order terms are needed. In a tokamak with up-down asymmetric equilibria second-order terms are required. For small $B_\theta/B \ll 1$ the dominant symmetry breaking mechanisms, as described in [3], are the slow radial variation of the plasma parameters, the slow poloidal variation of turbulence, finite orbit widths and neo-classical flows. A GS2 version that includes neo-classical corrections can model the effect on turbulence of neoclassical parallel velocity and heat flow, and neoclassical poloidal electric field [4-5]. Here GS2 was coupled with the neoclassical transport code NEO [8].

With no external momentum injection, the change of the ion rotation is determined by the total momentum conservation equation [5]:

$$\frac{\partial}{\partial t}\langle\langle n_i n_i R V_\zeta \rangle_\psi\rangle_T = \frac{1}{V'}\frac{\partial}{\partial \psi}(V'\Pi)$$

$$V' = \int d\theta d\zeta (\boldsymbol{B}.\nabla\theta)^{-1} \quad \text{Where}$$

$$\Pi = m_i \langle \langle \int d^3 v f_i R(\mathbf{v}\cdot\hat{\zeta})(\mathbf{v}\cdot\nabla\psi)\rangle_\psi\rangle_T$$

Π is the radial transport of ion toroidal angular momentum

V_ζ is the ion toroidal velocity

$d\zeta(.../\mathbf{B}\cdot\nabla\theta)$ is the flux surface average, $\langle ... \rangle_T$ is the average over several turbulence characteristic times and length scales, V' is the flux surface differential ,.

θ and ζ are the poloidal and toroidal angle, respectively, ψ is the poloidal magnetic flux, giving the magnetic field $\boldsymbol{B} = I\nabla\zeta + \nabla\zeta \times \nabla\psi$ where $I = B_\zeta R$ and B_ζ is the toroidal magnetic field.

INTRINSIC MOMENTUM FLUX

The effect of the flow and its gradient on the momentum transport can be linearized, giving an advective term and a diffusive term.

$$\Pi \simeq \Pi_{int} - P_\zeta n_i m_i \langle R^2\rangle_s \Omega_\zeta - \chi_\zeta n_i m_i \langle R^2\rangle_s \frac{\partial \Omega_\zeta}{\partial r},$$

P_ζ is the pinch coefficient, χ_ζ is the toroidal momentum diffusivity, and r is the radial coordinate.

$\Omega_\zeta = \Omega_{\zeta\,d} + \Omega_{\zeta\,E}$

where $\Omega_{\zeta,d}$ is the diamagnetic flow, and $\Omega_{\zeta\,E}$ the E × B plasma flow

Π_{int} is the intrinsic toroidal angular momentum flux in the absence of flow and flow shear

$\Pi_{int} = \Pi(\Omega_\zeta = 0, \partial\Omega_\zeta/\partial r = 0)$

In order to determine Π_{int}, we impose that both rotation and rotation shear are null:

$\Omega_\zeta = \Omega_{\nabla p} + \Omega_{\nabla T} + \Omega_{Er} = 0$ and $\partial/\partial r\,[\Omega_{\nabla p} + \Omega_{\nabla T} + \Omega_{Er}] = 0$.

$\Pi_{int} > 0$ expels positive (co-current) toroidal momentum, leaving counter-current momentum leading to hollow profiles.

GS2 INPUT:

Fig. 6. Four H discharges covering the LOC and SOC regimes. LOC-SOC transition at $n_e \sim 1.4x10^{-19} m^{-3}$.
(A)Low density with peaked rotation profile
(B) and (C) intermediate densities with hollow rotation
(D) high density with peaked rotation profile

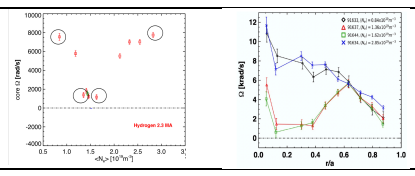

Fig.7 Measured plasma profiles and the smooth profiles input for simulations. Measured profiles from:
HRTS (n_e, Te)
H_α charge exchange spectrum (T_i, Ω)

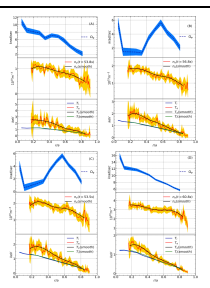

GS2 requires 2nd order gradients at the chosen flux surfaces

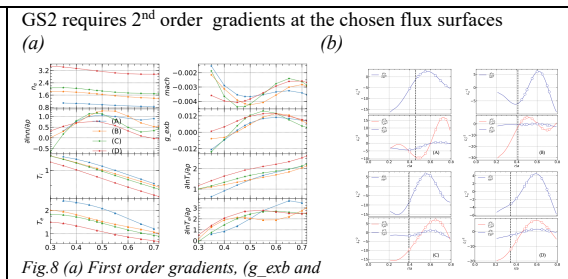

Fig.8 (a) First order gradients, (g_exb and mach are normalised diamagnetic shear and rotation); (b) 2nd order gradients

Calculated Momentum Fluxes

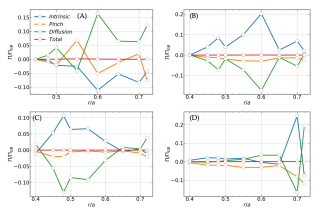

Fig. 9 GS2 calculated momentum fluxes (GS2 fluxes are in Gyro-Bohm units:

$$Q_{GS2} = \frac{Q}{n_T T_T v_{TT}} \rho^{*-2} \qquad \Pi_{GS2} = \frac{\Pi}{m_T n_T v_{TT}^2 a} \rho^{*-2}$$

Calculated turbulent Prandtl Number

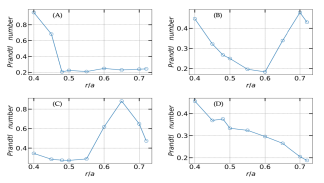

Fig.10- Prandtl Number (the ratio of momentum diffusivity X_ζ and the heat diffusivity χ_i): Pr = χ_ζ / χ_i with $\chi_i = \frac{Q_i}{n_i T_i / L_{T_i}}$

MODELLED ROTATION:

In steady state without external momentum sources, the radial momentum flux is zero at every flux surface. Π = 0 determines the radial profiles of the toroidal flow, $\Omega_\zeta(r)$

$$\Omega_\zeta(r) = \Omega_\zeta(a)\exp\left(\int_r^a \frac{P_\zeta(r')}{\chi_i(r')}\frac{1}{\Pr(r')}dr'\right)$$

$$-\int_r^a \left(\frac{\Pi_{int}}{Q_i}\frac{v_{T_i}}{R_0}\right)(r')\frac{1}{\Pr(r')}\frac{1}{2L_{T_i}(r')}\frac{v_{T_i}(r')}{R_0(r')}\exp\left(\int_r^{r'}\frac{P_\zeta(r'')}{\chi_i(r',)}\frac{1}{\Pr(r'')}dr''\right)dr'$$

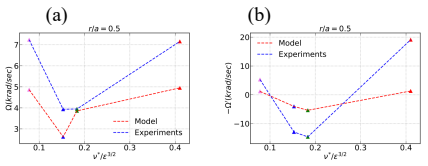

Fig. 11 – Measured and calculated (a) tor. angular freq. and (b) shear at r/a=0.5 vs ion-ion collision frequency $\nu^* = \nu_{ii} qR/v_{Ti}$

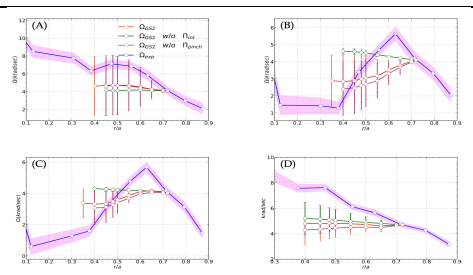

Fig.12 - Measured (Ω_{exp}) and reconstructed rotation profiles. In red: Ω_{GS2} including Π_{int} is based on the calculated change in rotation if the intrinsic momentum flux is balanced by diffusion and pinch terms. In green: Ω_{GS2} without Π_{int}. In magenta: Ω_{GS2} neglecting Pinch

The calculated Ω including Π_{int} give the correct signs (though not the amplitudes) for the rotation shear.
Without Π_{int} the calculated profiles for the mid-density cases (B, C) would be peaked, thus hollow profiles would not have been obtained.

CONCLUSION

Main ion rotation was measured in density scans of JET Ohmic plasmas, performed in H, D, T. Each isotope showed two rotation reversals [1].
Using a version of GS2 that includes neo-classical flows, non-linear modeling of the rotation profiles for one of the isotopes, H, was performed. The discharges modeled cover the whole density range and the typical profiles observed (peaked at low density, hollow for intermediate densities around and just after the LOC-SOC transition, peaked at high density). GS2 simulations had previously shown that as the $\nu^*_{ii} \sim n_i$ increases, the momentum flux reverses direction in qualitative agreement with the low-density rotation reversal observed in many tokamaks [4]. In the GS2 simulations shown here the model can simulate both rotation reversals, as the signs, but not the magnitude, of the modelled velocity gradients agree with observations of the rotation profiles measured at different densities. The model predicts velocity gradients smaller than those in the experiment. (Similar under-predictions have been reported for MAST [9] and ASDEX-U [10].) In all cases the change in rotation shear seems to be driven by the change in the shape of the density and temperature profiles, not the collisionality. Sensitivity studies are needed to confirm the robustness of the result. Finite orbit width effects not included in the calculation might also contribute significantly to the momentum flux (as might many other effects if the turbulence has a spatial scale as large as the poloidal Larmor radius).

REFERENCES

[1] MFF Nave et al. NF 63 (2023) 044002
[2] F.I. Parra and P.J. Catto P.J. 2010 PPCF 52 045004
[3] F.I. Parra, M. Barnes,P.J. Catto, NF 51 (2011) 113001
[4] M. Barnes et al, PRL 111, 055005 (2013).
*[5] J.P. Lee et al, PPCF **57** (2015) 125006*
[6] W. Dorland et al, PRL. 85, 5579 (2000).
[7] Camenen Y. et al 2017 PPCF 59 034001
[8] Staebler G.M., Kinsey J.E. and Waltz R.E. 2007 PoP. 14 055909
[9] Hillesheim J.C et al. 2015 NF 55 032003
[10] Hornsby W.A. et al, 2017 Nucl. Fusion 57 046008

This work has been carried out within the framework of the EUROfusion Consortium, funded by the European Union via the Euratom Research and Training Programme (Grant Agreement No 101052200 — EUROfusion). Views and opinions expressed are however those of the author(s) only and do not necessarily reflect those of the European Union or the European Commission. Neither the European Union nor the European Commission can be held responsible for them.